Analytical modeling of ground water level dynamics of tropical peatland drainage (Katingan Mentaya project area)

Cite as: AIP Conference Proceedings **2652**, 030007 (2022); https://doi.org/10.1063/5.0106453
Published Online: 14 November 2022

Albert Sulaiman, Desra Arriyadi, Taryono Darusman, et al.

Analytical Modeling of Ground Water Level Dynamics of Tropical Peatland Drainage (Katingan Mentaya Project Area)

Albert Sulaiman[1,a)], Desra Arriyadi[2)], Taryono Darusman[2)], Muhammad Irfan[3)], Guruh S. Ajie[4)], Titi Anggono[1)], Awaluddin[5)], Aryo Witono[2)], Syuhada[1)], Yan S. Chiqita[2)], Febty Febriani[1)], Cinantya N. Dewi[1)], Aditya D. Prasetio[1)], Mohammad Hasib[1)], Jeni Ricardo[2)], Dwi P. Lestari[2)]

[1]*Research Center for Physics, National Research and Innovation Agency (BRIN), Tangerang Selatan 15314, Indonesia*
[2]*PT Rimba Makmur Utama, Sampit, Central Kalimantan, Indonesia*
[3]*Department of Physics, Sriwijaya University, Ogan Komerling Ilir, Palembang, Indonesia*
[4]*Research Center for Lymnology, National Research and Innovation Agency (BRIN), Bogor 16911, Indonesia*
[5]*Technology Center for Disaster Risk Reduction, National Research and Innovation Agency (BRIN), Tangerang Selatan 15314, Indonesia*

[a)] *Corresponding author: albertus.sulaiman@brin.go.id*

Abstract. Peatlands have a unique hydrological system so that water management based on the peatland water system is a must. Peatland management by building drainage will cause changes in the structure of the peat, causing a high risk of forest fires, especially during the dry season. In this paper, we propose a model of tropical peatland drainage based on the 2D Darcy equation. With the initial and boundary conditions that we provide, the solution is solved using the expansion of the eigen-function. The simulation results show that the dynamics of the peat drainage water table is strongly influenced by rainfall rather than water input from the canal. There is a time lag between the rainfall and the increasing of the water table with the hydraulic coefficient determine the length of the time lag.

INTRODUCTION

Peatland has a unique hydrological system thereforea correct understanding will provide a correct water management. The introduction and arrangement of conservation and cultivation areas in peatlands based on a peatland water system or based on a peat hydrological unit is a must. In peatlands,water serves as a source of fresh water in large volumes. Under normal conditions, the volume of water in peat can reach 13 times the volume of the peat itself. Water is an important factor in the formation of peat domes and the absence of water will cause the peat to become brittle and flammable [1]. One of the important parameters in peatland water resource management is ground water level (GWL)[2].Lowering the ground water level (GWL) in peatlandswill cause carbon emissions as a result of the peat decomposition process [3].For cultivation purposes, the GWL is managed accordingly, providing suitable environment for the plants to survive[4]. However, managing the GWL is not an easy taskbecause peat has a high hydraulic coefficient both vertically and horizontally. Therefore, controlling the water level usinga canal network system becomes complicated. Important conditions should be considered carefully, such as the width of the canal, the depth of the canal and the sluice system. In this circumstance, modelling technology takes an essential part because with the model, we can develop various management scenarios.

Based on the water balanceconcept, the main inputs for water in peatlandscome from rainwater (precipitation), surface runoff from higher areas, and increasing GWLdue to the influence of the season or sea-level rise. Release of water in a peatlandsis influenced by surface flow system, seepage from the groundwater table, interception, and evapotranspiration [1]. The rate of natural water loss due to evapotranspiration, groundwater seepage, or surface runoff is not as fast as when peatlands are disturbed (drainage).Changes on the peat structure, such as caused by theconstruction of drainage channels, will disrupt the hydrological system (i.e., lowered the GWL), thatcauseshigh risk of forest fires, especially during the dry season [5,6]. Moreover, construction of drainage channels that reach the bottom of the dome will quickly drain the water to exit the peat system, and followed by

Proceedings of the 6th International Symposium on Frontiers of Applied Physics (ISFAP) 2021
AIP Conf. Proc. 2652, 030007-1–030007-11; https://doi.org/10.1063/5.0106453
Published by AIP Publishing. 978-0-7354-4264-1/$30.00

subsidence, causing the loss of its function as a water regulator. In this paper, scenarios of what will happen if peatlands are drained were studied based on analytical modelling of the peat water equilibrium equation.The analytical model of the dynamics of GWL in a canal peatland is obtained by solving the Darcy equation where this equation describes the behaviour of water content in a porous medium (such as peat). To find out the hydrological nature of the peatlands, we simulated GWL with three scenarios based on the water source, namely dry season conditions (without water input), the scenario of water input from canals and the water input from rain.

RESEARCH AREA

The study area is located in Central Kalimantan, Indonesia and flanked by the Mentaya River and the Katingan River. Currently, the concessionaire of this area is managed by PT. RimbaMakmur Utama (PT. RMU) that has been implementing restoration efforts since 2013 (see Figure (1)). In the case of simulating water table under intensive peatland drainage scenario, this area will be assumed as cultivation area.A canal, namelyHantipan canal (Figure(1a)) is located in the southern part of the project area and was established by the local government in 1992 as the main access that connecting Katingan River and Mentaya River [7]. Although the purpose of the canal is to provide alternative transportation for the surrounding villages, it also drains the water from the peat. The scenario of constructing a canal for water management is depicted in Figure(1b).At the site level, measurement have been taken place on six automatic water loggers in each piezometer that were installed along a 7 km transect perpendicular to the canal. The monitoring points were located in shrub area and forest area. Moreover, data from one weather station and one automatic water logger placed in the canal were also regularly monitored. The peat surface slope of the transect was measured using water hose method.

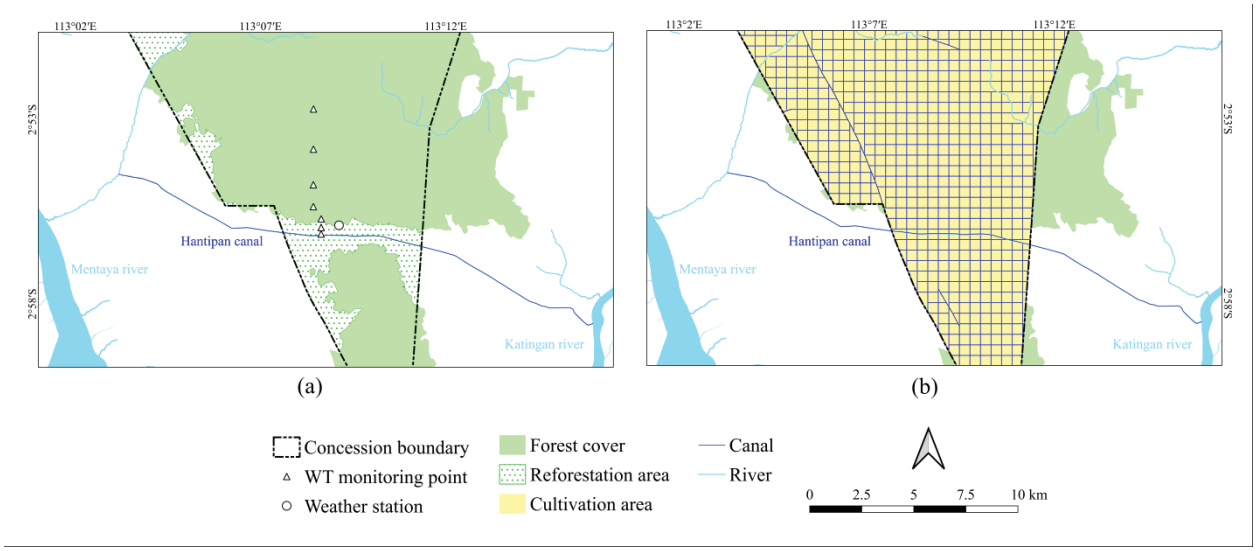

FIGURE 1. (a) Restoration project map with Hantipan Canal (blue line). (b) Drainage scenario map.

As the study area is located in the tropical zone, the climate is typically influenced by monsoonal with the annual rainfall approximately 2853 mm, annual mean temperature around 25.9 °C, and monthly mean evaporation patterns about 137 mm/day. Based on the field survey, peat depth is ranged from less than 2 m to more than 12 m[7]. Hydraulic conductivity in restoration area (no drainage) is ranged from about 0.01 m/day to around 0.1 m/day. For drainage scenario, a value of 0.5 m/day was used for the hydraulic conductivity.

THE GROUND WATER LEVEL MODEL

Peat is a dense medium with high porosity filled with water and air.Darcy's law is a general equation that used to state the transport of water level in a porous medium as a function of hydraulic conductivity and hydraulic gradient [8]. This law is applied to various forms of pore materials including soil and peat. Thus, the dynamics of GWL on peatlands fulfill the Darcy equation which could be used to explain the water balance equation on peatlands. To obtain an analytical solution, several assumptions were made. The first was the coefficient of the Darcy equation

known as the hydraulic conductivity which was assumed to be constant. Peat in the lateral and meridional directions is uniform,thus, only horizontal coordinate and time should be considered on this calculation. In this case, we used symbol*x, y*and *t* for zonal , meridionalandtime,respectively. Peat dome was ignored in this calculation as peat surface was assumed to be horizontal. Moreover, the canal has the same depth with the peat depth , thus, variations were only found as a function of time. The capillary effect was also neglected and the only source of water came from rainfall. If GWL is expressed in the function *h(x,t)* then Darcy's equation will be expressed in the form of [9],

$$\frac{\partial h}{\partial t}-\frac{\partial}{\partial x}\left(\kappa_x\frac{\partial h}{\partial x}\right)-\frac{\partial}{\partial y}\left(\kappa_y\frac{\partial h}{\partial y}\right)=f(t) \tag{1}$$

where κ is a coefficient called hydraulic conductivity and *f(t)* is a function of rainfall, evaporation and water in or out. The geometry of model is depicted in Figure 2.

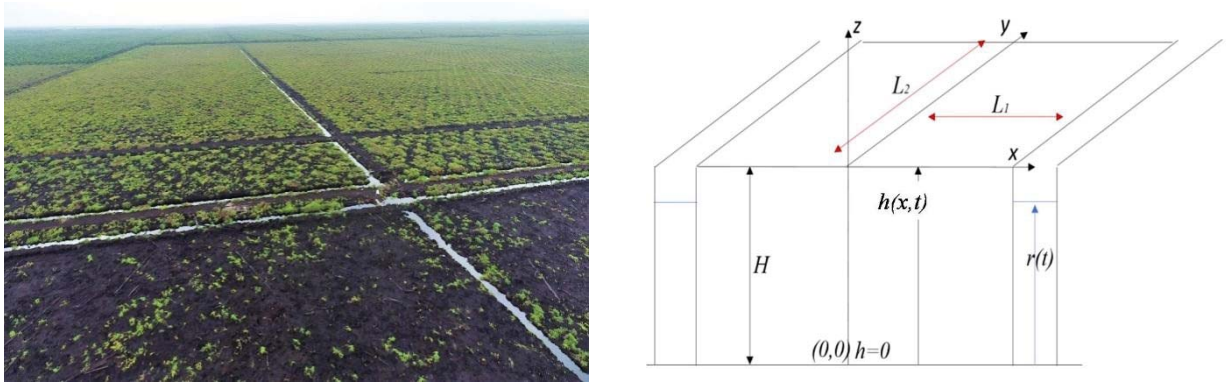

(a) (b)

FIGURE 2. Geometry of 2D peatland drainage.

The boundary value problems are,

$$\frac{\partial h(0,t)}{\partial x}=0 \quad ; \quad h(L_1,t)=r_1(t) \quad ; \quad \frac{\partial h(0,t)}{\partial y}=0 \quad ; \quad h(L_2,t)=r_2(t) \tag{2}$$

First, let us consider the homogeneous term i.e.*f(t)=0*, we can use the variable separation method as follows,

$$h(x,y,t)=a(t)\phi(x)\psi(y) \tag{3}$$

Substituting Eq. (3) into Eq. (1) with $f(t)=0$, yields,

$$\frac{1}{a}\frac{da}{dt}-\frac{\kappa_x}{\phi}\frac{d^2\phi}{dx^2}-\frac{\kappa_y}{\psi}\frac{d^2\psi}{dy^2}=0 \tag{4}$$

The second and third terms will produce the following eigenvalue equations,

$$\frac{d^2\phi_n(x)}{dx^2}=\lambda_n\phi_n(x) \quad ; \quad \frac{d^2\psi_m(y)}{dy^2}=\gamma_m\psi_m(y) \tag{5}$$

The eigenfunctions and their corresponding eigenvalues are,

$$\phi_n(x)=\cos\left(\frac{\lambda_n}{\sqrt{\kappa_x}}x\right) \quad ; \quad \psi_m(y)=\cos\left(\frac{\gamma_m}{\sqrt{\kappa_y}}y\right) \tag{6}$$

$$\lambda_n=(1+2n)\frac{\pi}{2L_1} \quad ; \quad \gamma_m=(1+2m)\frac{\pi}{L_2} \tag{7}$$

Now, we take the general solution of Eq. (1) in terms of,

$$h(x,y,t)=\sum_{m=0}^{\infty}\sum_{n=0}^{\infty}a_{nm}(t)\phi_n(x)\psi_m(y)+r(t) \tag{8}$$

Expanding Eq. (8) to the second order, we have,

$$\begin{aligned} h(x,y,t) &= a_0(t)\phi_0(x)\sum_n \psi_n(y) + a_1(t)\phi_1(x)\sum_n \psi_m(y) + r(t) + \ldots \\ &= a_0(t)\phi_0(x)\psi_0(y) + a_0(t)\phi_0(x)\psi_1(y) + a_1(t)\phi_1(x)\psi_0(y) + a_1(t)\phi_1(x)\psi_1(y) + r(t) \end{aligned} \tag{9}$$

Substituting Eq. (9) into Eq. (1) yields,

$$\begin{aligned} &\phi_0\psi_0\frac{da_0}{dt} + \phi_0\psi_1\frac{da_0}{dt} + \phi_1\psi_0\frac{da_1}{dt} + \phi_1\psi_1\frac{da_1}{dt} - \kappa_x a_0\psi_0\frac{d^2\phi_0}{dx^2} - \kappa_x a_0\psi_1\frac{d^2\phi_0}{dx^2} - \kappa_x a_1\psi_0\frac{d^2\phi_1}{dx^2} \\ &-\kappa_x a_1\psi_1\frac{d^2\phi_1}{dx^2} - \kappa_y a_0\phi_0\frac{d^2\psi_0}{dy^2} - \kappa_y a_0\phi_0\frac{d^2\psi_1}{dy^2} - \kappa_y a_1\phi_1\frac{d^2\psi_0}{dy^2} - \kappa_y a_1\phi_1\frac{d^2\psi_1}{dy^2} + \frac{dr(t)}{dt} = f(t) \end{aligned} \tag{10}$$

By using Eq. (6) we have,

$$\begin{aligned} &\phi_0\psi_0\frac{da_0}{dt} + \phi_0\psi_1\frac{da_0}{dt} + \phi_1\psi_0\frac{da_1}{dt} + \phi_1\psi_1\frac{da_1}{dt} + \kappa_x\lambda_0^2 a_0\phi_0\psi_0 + \kappa_x\lambda_0^2 a_0\phi_0\psi_1 + \kappa_x\lambda_1^2 a_1\phi_1\psi_0 \\ &+\kappa_x\lambda_1^2 a_1\phi_1\psi_1 + \kappa_y\gamma_0^2 a_0\phi_0\psi_0 + \kappa_y\gamma_1^2 a_0\phi_0\psi_1 + \kappa_y\gamma_0^2 a_1\phi_1\psi_0 + \kappa_y\gamma_1^2 a_1\phi_1\psi_1 + \frac{dr(t)}{dt} = f(t) \end{aligned} \tag{11}$$

If we multiply by ϕ_0 and integrate with respect to x for the integral boundary from $-L_1$ to L_1, we have

$$\begin{aligned} &\psi_0\frac{da_0}{dt}\int_{-L_1}^{L_1}\phi_0^2dx + \psi_1\frac{da_0}{dt}\int_{-L_1}^{L_1}\phi_0^2dx + \psi_0\frac{da_1}{dt}\int_{-L_1}^{L_1}\phi_0\phi_1dx + \psi_1\frac{da_1}{dt}\int_{-L_1}^{L_1}\phi_0\phi_1dx + \kappa_x\lambda_0^2 a_0\psi_0\int_{-L_1}^{L_1}\phi_0^2dx + \kappa_x\lambda_0^2 a_0\psi_1\int_{-L_1}^{L_1}\phi_0^2dx + \kappa_x\lambda_1^2 a_1\psi_0\int_{-L_1}^{L_1}\phi_0\phi_1dx \\ &+\kappa_x\lambda_1^2 a_1\psi_1\int_{-L_1}^{L_1}\phi_0\phi_1dx + \kappa_y\gamma_0^2 a_0\psi_0\int_{-L_1}^{L_1}\phi_0^2dx + \kappa_y\gamma_1^2 a_0\psi_1\int_{-L_1}^{L_1}\phi_0^2dx + \kappa_y\gamma_0^2 a_1\psi_0\int_{-L_1}^{L_1}\phi_0\phi_1dx + \kappa_y\gamma_1^2 a_1\psi_1\int_{-L_1}^{L_1}\phi_0\phi_1dx + \int_{-L_1}^{L_1}\phi_0\frac{dr(t)}{dt}dx = \int_{-L_1}^{L_1}\phi_0 f(t)dx \end{aligned} \tag{12}$$

With the integration properties and the boundary condition Eq. (2),

$$\begin{aligned} &\int_{-L_1}^{L_1}\phi_0^2dx = 2\int_0^{L_1}\cos^2\left(\frac{\lambda_0}{\sqrt{\kappa_x}}x\right)dx = 2\int_0^{L_1}\cos^2\left(\frac{\pi}{2L_1\sqrt{\kappa_x}}x\right)dx = \frac{4}{\pi}L_1\sqrt{\kappa_1}\int_0^{L_1}\cos^2(u)\,du \\ &= \frac{4}{\pi}L_1\sqrt{\kappa_1}\left(\frac{u}{2} + \frac{\sin 2u}{4}\Big|_0^{L_1}\right) = \frac{4}{\pi}L_1\sqrt{\kappa_1}\left(\frac{\pi x}{4L_1\sqrt{\kappa_x}} + \frac{1}{4}\sin\left(\frac{\pi}{L_1\sqrt{\kappa_x}}x\right)\Big|_0^{L_1}\right) = L_1 \end{aligned} \tag{13}$$

and

$$\begin{aligned} &\int_{-L_1}^{L_1}\phi_0\phi_1dx = 2\int_0^{L_1}\cos\left(\frac{\lambda_0}{\sqrt{\kappa_x}}x\right)\cos\left(\frac{\lambda_1}{\sqrt{\kappa_x}}x\right)dx = 2\int_0^{L_1}\cos\left(\frac{\pi}{2L_1\sqrt{\kappa_x}}x\right)\cos\left(\frac{3\pi}{2L_1\sqrt{\kappa_x}}x\right)dx \\ &= \frac{4}{\pi}L_1\sqrt{\kappa_1}\int_0^{L_1}\cos(\zeta)\cos(3\zeta)\,d\zeta = \frac{4}{\pi}L_1\sqrt{\kappa_1}\left[4\left(\frac{3\zeta}{8} + \frac{\sin 2\zeta}{4} + \frac{\sin 4\zeta}{32}\Big|_0^{L_1}\right) - 3\left(\frac{\zeta}{2} + \frac{\sin 2\zeta}{4}\Big|_0^{L_1}\right)\right] = 0 \end{aligned} \tag{14}$$

we arrive at the following equation,

$$\left[\psi_0 + \psi_1\right]\frac{da_0}{dt} + \left[\kappa_x\lambda_0^2\psi_0 + \kappa_x\lambda_0^2\psi_1 + \kappa_y\gamma_0^2\psi_0 + \kappa_y\gamma_1^2\psi_1\right]a_0 + \frac{1}{L_1}\int_{-L_1}^{L_1}\phi_0\left[\frac{dr(t)}{dt} - f(t)\right]dx = 0 \tag{15}$$

To obtain equation of motion of a_1, we multiply by ϕ_1 and integrate respect to x with integral boundary from $-L_1$ to L_1,

$$\psi_0 \frac{da_0}{dt}\int_{-L_1}^{L_2}\phi_0\phi_1 dx+\psi_1\frac{da_0}{dt}\int_{-L_1}^{L_2}\phi_0\phi_1 dx+\psi_0\frac{da_1}{dt}\int_{-L_1}^{L_2}\phi_1^2 dx+\psi_1\frac{da_1}{dt}\int_{-L_1}^{L_2}\phi_1^2 dx+\kappa_x\lambda_0^2 a_0\psi_0\int_{-L_1}^{L_2}\phi_0\phi_1\,dx+\kappa_x\lambda_0^2 a_0\psi_1\int_{-L_1}^{L_2}\phi_0\phi_1\,dx+\kappa_x\lambda_1^2 a_1\psi_0\int_{-L_1}^{L_2}\phi_1^2 dx$$
$$+\kappa_x\lambda_1^2 a_1\psi_1\int_{-L_1}^{L_2}\phi_1\,dx+\kappa_y\gamma_0^2 a_0\psi_0\int_{-L_1}^{L_2}\phi_0\phi_1\,dx+\kappa_y\gamma_1^2 a_0\psi_1\int_{-L_1}^{L_2}\phi_0\phi_1\,dx+\kappa_y\gamma_0^2 a_1\psi_0\int_{-L_1}^{L_2}\phi_1^2 dx+\kappa_y\gamma_1^2 a_1\psi_1\int_{-L_1}^{L_2}\phi_1^2 dx+\int_{-L_1}^{L_2}\left[\frac{dr(t)}{dt}-f(t)\right]\phi_1 dx=0$$

We solve the integration as follows,

$$\int_{-L_1}^{L_1}\phi_1^2 dx=2\int_0^{L_1}\cos^2\left(\frac{\lambda_1}{\sqrt{\kappa_x}}x\right)dx=2\int_0^{L_1}\cos^2\left(\frac{3\pi}{2L_1\sqrt{\kappa_x}}x\right)dx=\frac{2}{3\pi}L_1\sqrt{\kappa_1}\left(\frac{3\pi}{4L_1\sqrt{\kappa_x}}x+\frac{1}{4}\sin\left(\frac{3\pi}{L_1\sqrt{\kappa_x}}x\right)\Bigg|_0^{L_1}\right)=\frac{L_1}{2} \tag{16}$$

By using Eq. (14) and Eq. (16), we arrive at the following equation,

$$\left(\psi_0+\psi_1\right)\frac{da_1}{dt}+\left[\kappa_x\lambda_1^2\psi_0+\kappa_x\lambda_1^2\psi_1+\kappa_y\gamma_0^2\psi_0+\kappa_y\gamma_1^2\psi_1\right]a_1+\frac{2}{L_1}\int_{-L_1}^{L_2}\left[\frac{dr(t)}{dt}-f(t)\right]\phi_1 dx=0 \tag{17}$$

Eq. (15) and Eq. (17) can be written as follows,

$$\left[\psi_0+\psi_1\right]\frac{da_0}{dt}+\left[\left(\psi_0+\psi_1\right)\kappa_x\lambda_0^2+\kappa_y\gamma_0^2\psi_0+\kappa_y\gamma_1^2\psi_1\right]a_0+\frac{1}{L_1}\int_{-L_1}^{L_1}\phi_0\Gamma(t)dx=0 \tag{18}$$

$$\left[\psi_0+\psi_1\right]\frac{da_1}{dt}+\left[\left(\psi_0+\psi_1\right)\kappa_x\lambda_1^2+\kappa_y\gamma_0^2\psi_0+\kappa_y\gamma_1^2\psi_1\right]a_1+\frac{2}{L_1}\int_{-L_1}^{L_2}\phi_1\Gamma\left(t\right)dx=0 \tag{19}$$

where

$$\Gamma(t)=\frac{dr(t)}{dt}-f(t) \tag{20}$$

Similarly, integrating with respect to the function ψ, we get,

$$\left[\phi_0+\phi_1\right]\frac{da_0}{dt}+\left[\left(\phi_0+\phi_1\right)\kappa_x\lambda_0^2+\kappa_y\gamma_0^2\phi_0+\kappa_y\gamma_1^2\phi_1\right]a_0+\frac{2}{L_1}\int_{-L_1}^{L_1}\psi_0\Gamma(t)dx=0 \tag{21}$$

$$\left[\phi_0+\phi_1\right]\frac{da_1}{dt}+\left[\left(\phi_0+\phi_1\right)\kappa_x\lambda_1^2+\kappa_y\gamma_0^2\phi_0+\kappa_y\gamma_1^2\phi_1\right]a_1+\frac{2}{L_1}\int_{-L_1}^{L_2}\psi_1\Gamma\left(t\right)dx=0 \tag{22}$$

Since the functions $\phi(x)$ and $\psi(y)$ are functions of x and y, then for $a(t)$ they are constants. The equation of $a(t)$ has general form as,

$$\frac{da_\alpha}{dt}+\Omega_\alpha\left(\phi_n,\psi_m\right)a_\alpha=\Theta_\alpha(t)\quad,\quad \Theta_\alpha(t)=-\bar{L}_\alpha\int_{-L_1}^{L_2}\Upsilon_\alpha\left(\phi_n,\psi_m\right)\Gamma\left(t\right)dx \tag{23}$$

with α=0,1,2,...

If we multiply by using $exp(\Omega_\alpha(\phi,\psi)t)$ for both sides, we get,

$$\left(\frac{da_\alpha}{dt}+\Omega_\alpha\left(\phi_n,\psi_m\right)a_\alpha\right)e^{\Omega_\alpha t}=\Theta_\alpha(t)e^{\Omega_\alpha(\phi_n,\psi_m)t}\quad\rightarrow\quad\frac{d}{dt}\left(a_\alpha(t)e^{\Omega_\alpha(\phi_n,\psi_m)t}\right)=\Theta_\alpha(t)e^{\Omega_\alpha(\phi_n,\psi_m)t} \tag{24}$$

Then, we have the solution for $a(t)$ as,

$$a_\alpha\left(t\right)=e^{-\Omega_\alpha(\phi_n,\psi_m)t}\int_t\Theta_\alpha(\tau)e^{\Omega_\alpha(\phi_n,\psi_m)\tau}d\tau \tag{25}$$

The general solution of Eq. (1) is given by,

$$h\left(x,y,t\right)=\sum_{\alpha=0}^{\infty}\sum_{n=0}^{\infty}\sum_{m=0}^{\infty}A_{nm}\cos\left(\frac{\lambda_n}{\sqrt{\kappa_x}}x\right)\cos\left(\frac{\gamma_m}{\sqrt{\kappa_y}}y\right)e^{-\Omega_\alpha(\phi,\psi)t}\int_t\Theta_\alpha(\tau)e^{\Omega_\alpha(\phi,\psi)\tau}d\tau \tag{26}$$

where the form of $r(t)$ is determined by the initial condition. This is a water table dynamics solution for two-dimensional canals.The equation is used as the basis for simulating the dynamics of GWL in peatlands. We develop three scenarios for simulations performed with Matlab.

RESULTS AND DISCUSSION

Field Measurement in Restoration Project

To ignore the influence of precipitation, only water level data during dry spell (no rainfall)were used to describes the GWL profile. In 2019, a long dry spell were recordedin the study area from 22 July 2019 to 29 September 2019,with$t$= 67 days. In drainage scenario, x = 0 describes the highest point of the cross-section between two canals and the middle between -L and L. Whereas in restoration project, x = 0 cannot be defined because it only has one existing canal. The groundwater flow direction assumed through towards the canal was showed on Figure 3(a).

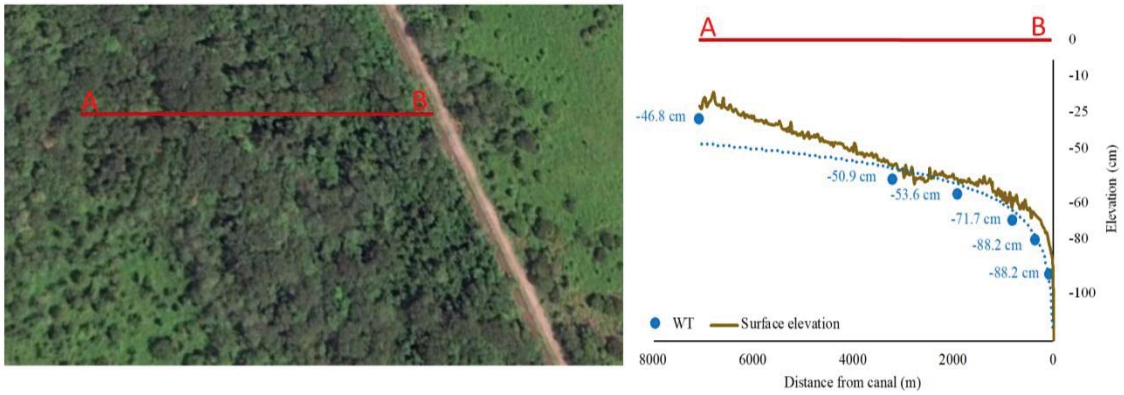

(a) (b)

FIGURE 3. (a) An existing canal in restoration area. (b) Side view of average water level during a dry spell period in 2019 from six piezometers.

Figure 3(b) shows the average GWL curve of measured piezometers. It is clear that GWL decreases as increasing distance from the canal. The nearest monitoring point to the canal has lowest GWL at -88.2 cm, while the GWL at the farthest monitoring point was -46.8 cm. The plot of GWL and distance from the canal resulted logarithmic trend with R^2 value was 0.86. The steep curve of GWL found around 0-500 m to the canal.

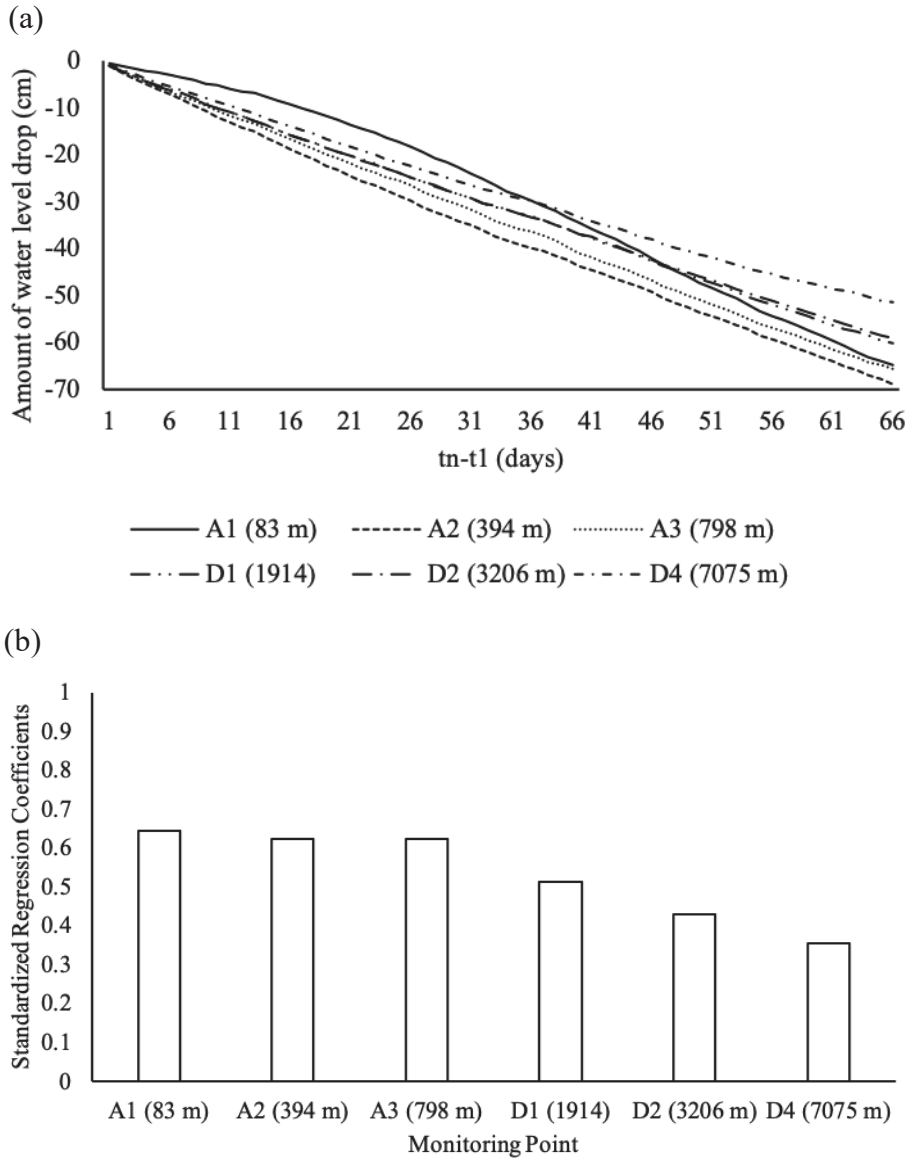

FIGURE 4. (a) Water level decrease from $h(x,1)$ as initial value for different distance from canal. (b) GWL decrease from $h(x,1)$ as initial value for different distance from canal, where A are monitoring points on shrub area and B were located on forest area.

The results of the GWL daily decrease from six piezometers are depicted in Figure4a. Water loss from peatland system during dry spell were caused by evapotranspiration and ground flow of water. In the graph, the drop ofGWLwere plotted against time with no rainy days in 2019. Data at t =1 was used for initial value. The results show the difference between initial value and the data at the end of the period (t = 67).The GWL at the end of the period for the monitoring points locatedon shrub area(A1, A2, and A3) ranged from -65 cm to -70 cm, while those located on forest area (D1, D2, and D4) ranged from -50 cm to -60 cm. Another important result is the average of the daily GWL decrease from all piezometers was 0.9±0.2 cm/day during that period.

As one of the input for peat water, rainfall directly affects the fluctuation of GWL. The sensitivity of GWL to rainfall was calculated using Standardized Regression Coefficient (SRG)$SRG_i=b_i\ SD(x)/SD(y_i)$where b_i is regression coefficient, $SD\ (x)$is standard deviation of rainfall, and $SD\ (y_i)$is standard deviation of the amount of GWLincrease.Figure4b shows the SRG values on each monitoring point. Groundwater response on shrub area to

rainfall was higher than groundwater response on forest area. SRG value in shrub area was around 0.6, while in forest, the SRG value ranged from 0.3 to 0.5. Unlike the shrub area, rainfall that reached the surface of forest floor was affected by interception which causes water being evaporated from plant surface back to the atmosphere.Thus,the net rainfall in forest floor area was less than shrub area.

Analytical Modeling in Drainage Scenario

Following the scenario of the intensive drainage, common practices were laid out in a step wise to make canal connections. There are three types of canals, primary canal that enclose the concession areas, secondary canal as discharging into main canals, and tertiary canal as planting block border. For this research, the dynamics of GWL was simulated only for tertiary canals, in order to simplify the actual situation. In this simulation, the time interval was expressed in days. We usedthe hydraulic coefficient of 0.5m/day. The source term consists of rainfall c(t) and water input from canals with river water levels fluctuate periodically with the following functions [10] ,

$$r(t)=\frac{H}{2}\left[\cos\left(\frac{\pi}{T}t\right)+1\right] \tag{27}$$

where T is the time for the river to dry up. In this paper, we simulated three scenarios, first was the scenario of dry season i.e. the conditions without rain. In this scenario, the day without rain in the study area was 208 days. The second scenario was a simulation without rain but there was a water input from the canal which was modelled as $r(t)=H/2\ exp(-(t-t_0)^2/\sigma)[cos(\pi t/T)+1]$. The third scenario was that there was rain in a certain period. The function of rainfall intensity over time generally resembles a distribution function as in statistics where the Gaussian function is dominant in the tropic.If the precipitation is taking into account, we use Gaussian model as follow [11],

$$f(t)=f_0 e^{-\frac{(t-t_0)^2}{2\sigma^2}} \tag{28}$$

with σ is standard deviation of Gaussian curve.

The simulation results for the three scenarios are depicted in Figure5. The first scenario Figure5a shows that the209 days of dry spell caused the GWL of peatland located in two canals which200m apart will be degraded down from 0 to 2m by 40m. The water in the canal with a depth of 2 meters will dry with the wet peat dome is 120m long. Meanwhile, for the second scenario where there was water input from rivers/canals with a maximum discharge of around 0.33m^3/s with a Gaussian distribution, it produced a profile that was not much different from dry condition. Furthermore, if there is rainfall with an amplitude of 30mm with a Gaussian distribution for 20 days, the peat dome will remain wet as far as 160m or about 80% of the total peat area. These results indicate that water input from rivers does not have a significant impact on water content in peatland but rainfall does. This gives evidence that the main source of water for peatland is rainfall.

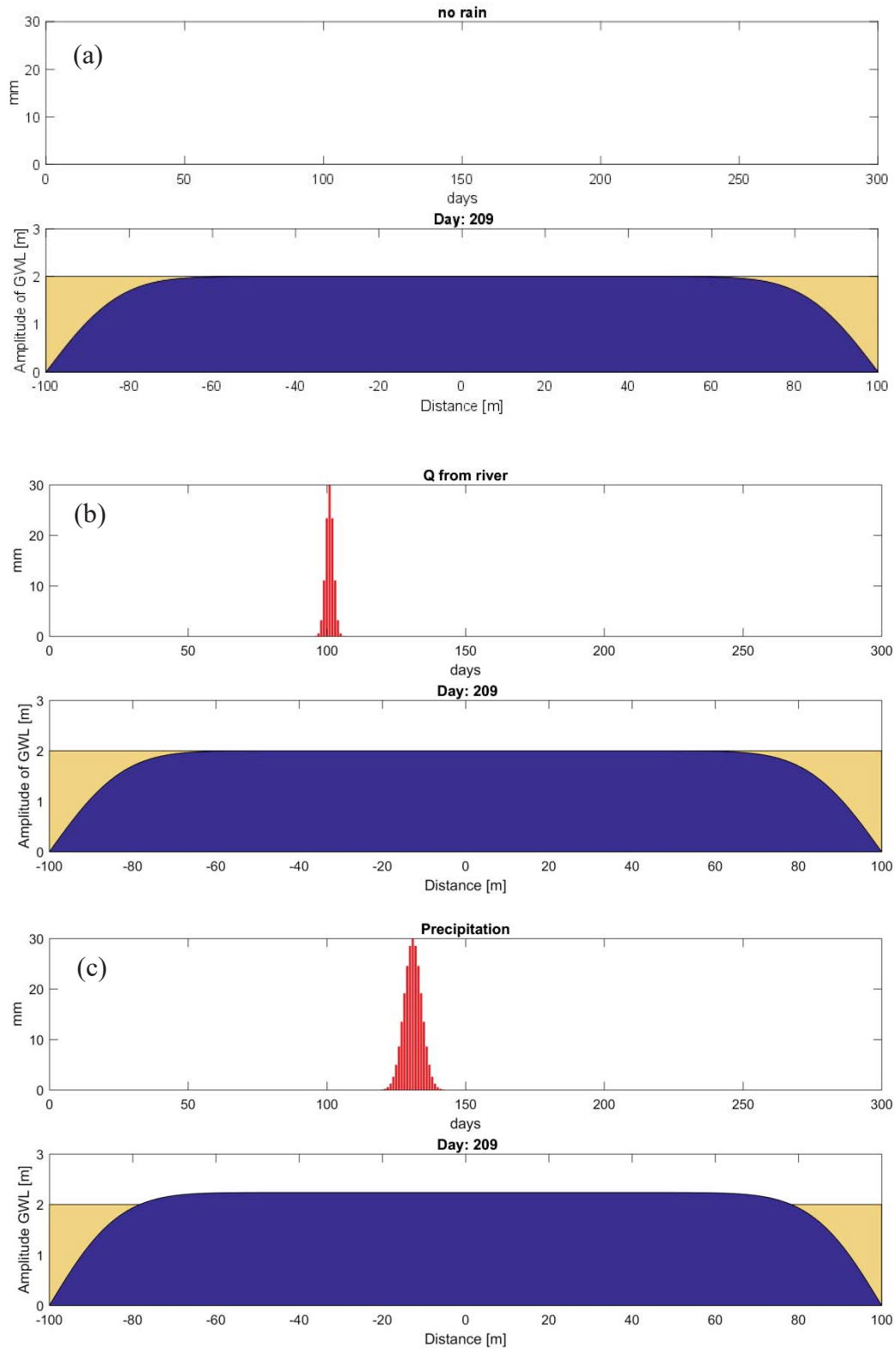

FIGURE 5. (a) The shape of GWL for peatlandin condition without rain (b) The shape of the GWL for peatlands with water mass input from rivers/canals (c) The shape of the GWL for peatland with water mass input from rainfall.

The dynamic scenario of peatland GWL for one year is depicted in Figure6. For the no rain scenario, the GWL of a peatland with an area of 60,000 m^2 is expressed in Figure6a. It clearly explained that the GWL in the peat dome will drop by more than 0.5m. A decrease in GWL of more than 0.5m will make the peat to be prone to fire [12] and emit carbon into the atmosphere [4]. If in one year there is rain with a high intensity of more than 30m in about 50 days (following the Gaussian distribution which is an ideal condition) then the peat dome will remain wet and allow flooding to occur. The dependence of peatland GWL on rainfall shows that peatlands are very vulnerable to climate change. When GWL decreases, peat emits carbon which contributes to global warming [1].Moreover, if peat is burned, the contribution of global warming will increase many times. So there is feedback between the dynamics of the GWL and climate change where this feedback mechanism is still an open.

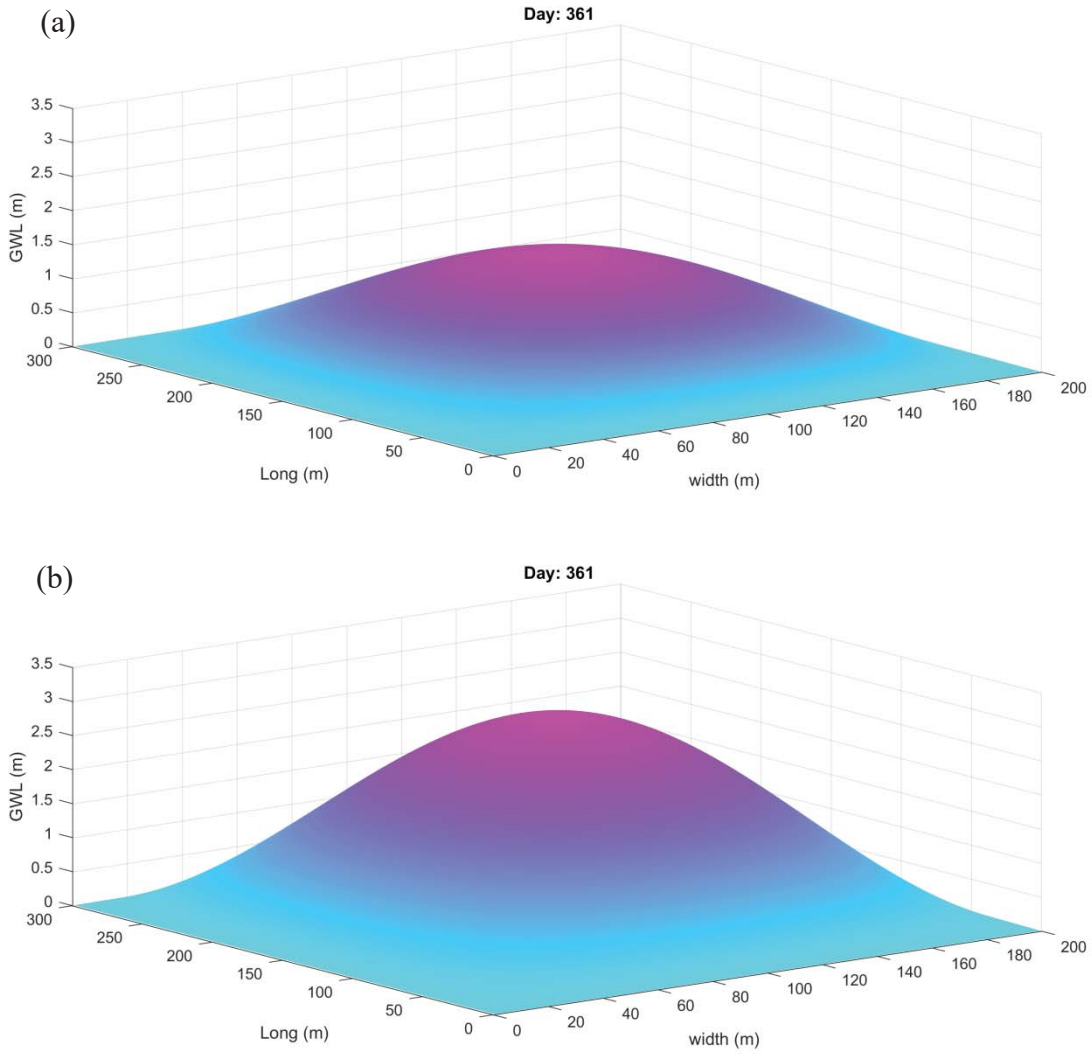

FIGURE 6. (a) The peat doom at the dry season (b) The peat doom at the wet season.

CONCLUSION

The modelling of GWL dynamics on peatlands with canalized peat conditions has been carried out. We assume that peat is a homogeneous medium so that the coefficient of hydraulic conductivity is considered constant throughout the peatland area. The solution is obtained by using the expansion of the eigen-functions.. We used three scenarios to predict the behavior of GWL, namely conditions without rain, conditions with water mass input from rivers (canals) and conditions with rain. The results show that the presence of water from the canal is not significant for peat wetting but comes from rainfall. This indicates that the water source in peatlands is significantly derived from

rainwater. This implies that during dry season, the most effective way to maintain the GWL is by holding back the water so it will not disappear. One of the engineering that can be done is the construction of canal blocking.

ACKNOWLEDGMENTS

This research was funded by P2F LIPI and PT RMU for the 2021 fiscal year.

REFERENCES

1. M. Osaki and N. Tsuji,*Tropical Peatland Ecosystems* Springer Verlag, Berlin (2016).
2. M. Taufik, A. A. Veldhuizen, J. H. M. Wosten, H. A. J. Lanen, Geoderma **347,** 160–169 (2019).
3. T. Hirano, K. Kusin, and M. Osaki, Glob. Chang. Biol. **20**, 555–565 (2014).
4. S. Sundari, T. Hirano, H. Himada, K. Kusin and S. Limin, J. Agric. Meteorol. **68**, 121–134 (2012).
5. A. Rossita, A. Witono, T. Darusman, D.P. Lestari DP, I. Risdiyanto, IOP Conf. Ser.: Earth Environ. Sci. **129**, 012001 (2018).
6. M. Mezbahuddin, R.F. Grant, and T. Hirano, Biogeosciences **11**, 577–599, (2014).
7. M. Bloomestijn, Water retention for peatland restoration in Central Kalimantan as part of the Katingan Project, Wageningen University and Research, (2017).
8. S. L. Dingman, Physical Hydrology: Third Edition, Long Grove, Illinois (2015).
9. A. R Cobb,A. M. Hoyt , L. Gandois , J. Erid , R. Dommain , K. A.Salimg , F. M. Kai, N. S. Haji Su'uth , and C. F. Harveya, Proc. Natl. Acad. Sci. **114,** E5187–E5196 (2017).
10. J. Noordermeer, B.Sc. thesis, Twente University, 2010.
11. H. Sauvageot, J. Appl. Meteor. **33**, 1255–1263 (1994).
12. E. I. Putra, M. A. Cochrane, Y. Vetrita, L. Graham, and B. H. Saharjo, 15th International Peat Congress (2016).